Singly *anti-anti* Carboxylate-Bridged Zig-Zag Chain Complexes from a Carboxylate-Containing Tridentate Schiff Base Ligand and $M(hfac)_2$ [M = Mn^{II}, Ni^{II}, and Cu^{II}]: Synthesis, Crystal Structure, and Magnetic Properties

Enrique Colacio,*[a] Jose M. Domínguez-Vera,[a] Mustapha Ghazi,[a] Raikko Kivekäs,[b] Martti Klinga,[b] and José M. Moreno[a]

Keywords: Copper / Nickel / Manganese / Carboxylate bridge / Metal complexes / Magnetic properties

The reaction of $M(hfac)_2$ with the tridentate Schiff base H_2L (where H_2L stands for the 1:1 condensation product of 2-imidazolecarboxaldehyde with β-alanine) leads to the complexes $[M(HL)(hfac)]_n$ [M = Mn^{II}, Ni^{II}, and Cu^{II}; hfac = hexafluoroacetylacetonate anion] (**1**–**3**). The structures of the complexes **1** and **3** have been solved by X-ray crystallographic methods. The structures are very similar and consist of infinite zig-zag chains, running parallel to the *b* axis, in which the metal ions are bridged sequentially by *anti-anti* carboxylate groups with intrachain metal–metal distances of 6.134 Å for **1** and 6.239 Å for **3**. Each monodeprotonated HL ligand acts as a tridentate one to a metal(II) ion and as a monodentate one to a neighbouring metal(II) centre. Metal atoms exhibit distorted octahedral coordination spheres comprised of two oxygen atoms from the hexafluoroacetylacetonate ligand, three donor atoms from the HL ligand and the oxygen atom belonging to the carboxylate group of an adjacent molecule. The complexes **1–3** have been confirmed to be isomorphous and isostructural on the basis of X-ray powder diffraction and IR spectra. The magnetic properties of the three compounds were studied by susceptibility measurements as a function of the temperature and successfully analyzed in terms of the isotropic spin Hamiltonian for one-dimensional infinite chain systems to give the coupling parameters J = –0.91 cm^{-1}, g = 2.03 (**1**); J = –13.2 cm^{-1}, g = 2.24 (**2**); and J = 0.40 cm^{-1}, g = 2.11 (**3**). The magnetic behaviour for all three complexes can be satisfactorily explained in terms of the conformation of the bridge and the interaction between the d orbitals of the metal centre and the bridge.

Polynuclear complexes containing bridging carboxylate groups are of current interest due to the fact that the carboxylate ions play a key role as a ligand in many biochemical systems involving mono- and polymetallic active sites.[1,2] In addition, polynuclear metal carboxylates are good candidates for the investigation of exchange-coupling interaction between adjacent metal ions.[3–6] Carboxylate is a versatile anion that can assume many types of bridging conformations, the most important being monoatomic and triatomic *syn-syn*, *syn-anti*, and *anti-anti*[5,6] (see Scheme 1). Copper(II) complexes with monoatomic or *syn-anti* triatomic conformations exhibit very weak magnetic exchange interactions,[5,7] whereas triatomic *syn-syn* and *anti-anti* conformations mediate large and weak to medium antiferromagnetic interactions, respectively.[8,9] Among metal(II) carboxylate polymers, structurally and magnetically characterized singly carboxylate-bridged chain complexes are rare[4,10–12] and those adopting the *anti-anti* conformation are rarer still. To our knowledge, they are limited to three Mn^{III} Schiff base chain complexes[11,13,14] and one Fe^{II}[15] and one Cu^{II}[9] two-dimensional complex.

Polydentate ligands with carboxylate groups are good candidates to undergo self-assembly processes based on complexation reactions. In fact, we have previously shown that the tridentate ligand 1,3-dimethyl-5-[(2-carboxyphen-

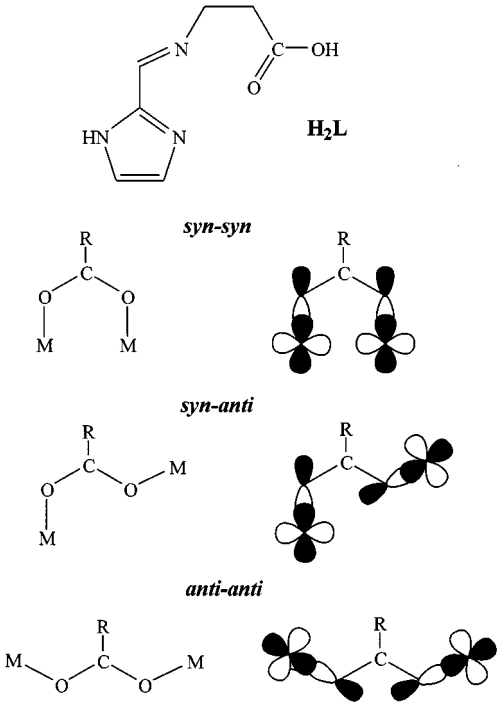

Scheme 1. The H_2L ligand and some of the bridging conformations for the carboxylate group

[a] Departamento de Química Inorgánica, Universidad de Granada, Facultad de Ciencias, E-18071 Granada, Spain
[b] Department of Chemistry, Laboratory of Inorganic Chemistry, P.O. Box 55, FIN-00014 University of Helsinki, Finland

  1434–1948/99/0303–0441 $ 17.50+.50/0

yl)azo]barbituric acid reacts with copper(II) leading to a *syn-anti* carboxylate-bridged helix chain copper(II) complex through a self-assembly reaction.[4] Following a similar strategy we succeeded in obtaining a series of *anti-anti* singly carboxylate-bridged chain complexes from the reaction of the precursors $M(hfac)_2$ [M = Mn^{II}, Ni^{II}, and Cu^{II}, hfac = hexafluoroacetylacetonato anion] with the tridentate Schiff base H_2L, where H_2L stands for the 1:1 condensation product of 2-imidazolecarboxaldehyde and β-alanine (see Scheme 1). The present paper is devoted to the structural and magnetochemical studies of these complexes.

When the square-planar complexes $M(hfac)_2$ [M = Mn^{II}, Ni^{II}, and Cu^{II}] react with the tridentate Schiff base H_2L, the ligand loses the carboxylic proton and replaces one of the hfac ligands of the precursor complex to give rise, in principle, to a pentacoordinated complex. Because the metal ion is able to additionally receive the non-coordinated oxygen atom of the carboxylate group belonging to another pentacoordinated molecule, a spontaneous self-assembly reaction occurs leading to singly carboxylate-bridged chain complexes $[M(HL)(hfac)]_n$. It should be pointed out that chemical analyses, IR spectra and powder X-ray data confirm that compounds **1**−**3** are isomorphous and isostructural.

Crystal Structures

Complexes **1** and **3** are isostructural and consist of infinite zig-zag chains, running parallel to the *b* axis, in which the metal ions are bridged sequentially by *anti-anti* carboxylate groups. A perspective view of the zig-zag chain for **3**, together with the corresponding atom labelling scheme, is given as an example in Figure 1. Selected bond lengths and angles are listed in Table 1.

Each monodeprotonated HL ligand acts as a tridentate one to a metal(II) ion and as monodentate one to a neighbouring metal(II) centre. Metal atoms exhibit distorted octahedral coordination spheres comprised of two oxygen atoms from the hexafluoroacetylacetonate ligand, three donor atoms from the HL ligand, and the oxygen atom belonging to the carboxylate group of an adjacent molecule. As expected, the three donor atoms of HL occupy in-plane coordination positions and then the carboxylate bridges have to be oriented in a mutually *cis* fashion. The tridentate behaviour of the HL ligand results in the formation of one five- and one six-membered rings having the M−N(7) bond in common. For **3**, the *anti-anti* carboxylate group bridges two Cu^{II} ions in equatorial-axial positions and the surrounding of each copper ion is (4+2), the octahedron being elongated along the O(17)−Cu(1)−$O(12)^{ii}$ axis (*ii* = 1 − *x*, 0.5 + *y*, 1.5 − *z*). In the M−O−C−O−M fragment of **3**, the metal ions are pushed out of the COO plane by 0.214 and 0.806 Å. In **1** the metal ions are also out of the COO plane by 0.620 and 0.652 Å. For both compounds large deviations from the idealized orthogonal geometry are found at the metal atom in the five-membered M−N(1)−C(2)−C(6)−N(7)−M rings [N(1)−Mn−N(7) = 74.33(18)° for **1** and N(1)−Cu−N(7) = 81.45° for **3**]. Such deviations are expected to be due to the small bite distance of this part of the HL ligand. Bond lengths of M(hfac) moieties are in agreement with those reported for other hfac-

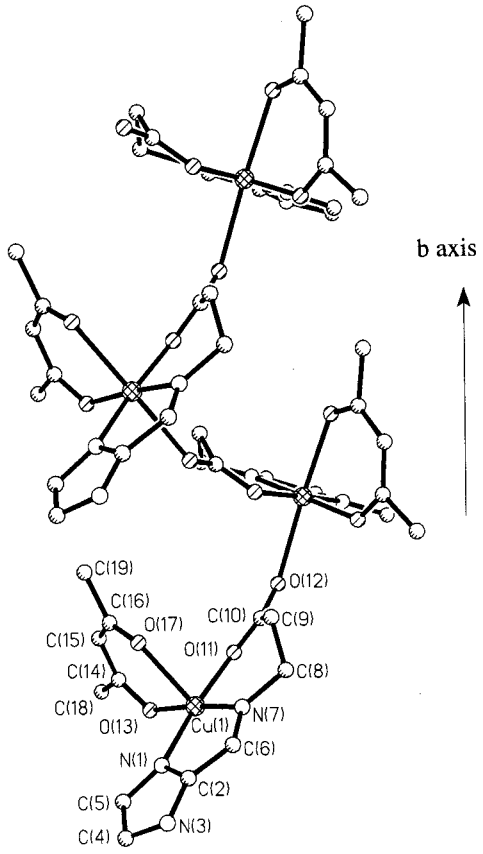

Figure 1. Perspective view of complex **3** along the *b* axis

Table 1. Selected bond lengths [Å] and angles [°] for **1** and **3**

Complex **1**			
Mn(1)−$O(12)^{i}$	2.111(5)	Mn(1)−O(17)	2.218(5)
Mn(1)−O(13)	2.134(4)	Mn(1)−N(1)	2.230(5)
Mn(1)−O(11)	2.142(5)	Mn(1)−N(7)	2.262(5)
$O(12)^{i}$−Mn(1)−O(13)	91.90(17)	O(11)−Mn(1)−N(1)	156.59(18)
$O(12)^{i}$−Mn(1)−O(11)	89.15(18)	O(17)−Mn(1)−N(1)	93.42(18)
O(13)−Mn(1)−O(11)	101.64(17)	$O(12)^{i}$−Mn(1)−N(7)	92.39(19)
$O(12)^{i}$−Mn(1)−O(17)	172.84(17)	O(13)−Mn(1)−N(7)	174.24(18)
O(13)−Mn(1)−O(17)	81.61(16)	O(11)−Mn(1)−N(7)	82.28(18)
O(11)−Mn(1)−O(17)	89.21(19)	O(17)−Mn(1)−N(7)	94.29(18)
$O(12)^{i}$−Mn(1)−N(1)	90.85(18)	N(1)−Mn(1)−N(7)	74.33(18)
O(13)−Mn(1)−N(1)	101.76(18)		
Complex **3**			
Cu(1)−O(11)	1.933(3)	Cu(1)−N(7)	2.007(3)
Cu(1)−O(13)	1.969(3)	Cu(1)−O(17)	2.359(3)
Cu(1)−N(1)	1.984(3)	Cu(1)−$O(12)^{ii}$	2.446(3)
O(11)−Cu(1)−O(13)	91.80(12)	N(1)−Cu(1)−O(17)	94.41(13)
O(11)−Cu(1)−N(1)	173.05(12)	N(7)−Cu(1)−O(17)	96.15(12)
O(13)−Cu(1)−N(1)	94.70(13)	N(1)−Cu(1)−$O(12)^{ii}$	88.60(12)
O(11)−Cu(1)−N(7)	91.99(12)	N(7)−Cu(1)−$O(12)^{ii}$	89.64(12)
O(13)−Cu(1)−N(7)	175.92(13)	O(11)−Cu(1)−$O(12)^{ii}$	89.06(12)
N(1)−Cu(1)−N(7)	81.46(13)	O(13)−Cu(1)−$O(12)^{ii}$	88.89(11)
O(11)−Cu(1)−O(17)	88.55(14)	O(17)−Cu(1)−$O(12)^{ii}$	173.81(9)
O(13)−Cu(1)−O(17)	85.48(11)		

i = 1 − *x*, 0.5 + *y*, 0.5 − *z*; *ii* = 1 − *x*, 0.5 + *y*, 1.5 − *z*.

containing Mn^{II} and Cu^{II} complexes.[16] The *anti-anti* bridging mode for **3** affords an intrachain metal−metal distance of 6.239 Å, whereas for **1** the metal−metal distance is 6.134 Å; they are similar to those found for singly *anti-anti* carboxylate-bridged Mn^{III}[11,13,14] and Fe^{III}[15] complexes. The shortest interchain metal separations are 7.412 and 6.854 Å for **1** and **3**, respectively. The polymeric chains are held together by pairs of complementary hydrogen bonds between the N(3)−H group and the carboxylate oxygen atoms of a neighbouring chain.

Magnetic Properties

The EPR spectrum of complex **1** at 100 K exhibits a featureless broad resonance at $g = 2.00$ with a half-height width of 400 G. The broadness of this EPR signal is characteristic of polynuclear manganese(II) complexes. The frozen methanol solution spectrum at 100 K exhibits an allowed hyperfine sextuplet centred at $g = 2.0$ ($A = 88.10^{-4}$ cm^{-1}) with forbidden hyperfine lines corresponding to transitions between levels with different nuclear magnetic quantum numbers. This spectrum is typical of electronically isolated Mn^{II} species, thus suggesting either that the chain structure of complex **1** is not retained in solution or that the small antiferromagnetic interaction operating between the Mn^{II} ions does not modify appreciably the EPR spectrum of the complex. Neither polycrystalline powder nor solution EPR spectra could be detected for complex **2**. At 100 K the spectrum of a polycrystalline sample of **3** looks like that expected for a copper(II) ion in a d(x^2-y^2) ground state. Two main features are attributable to paralell ($g_{||} = 2.24$) and perpendicular ($g_{\perp} = 2.11$) components of an axially symmetrical spectrum. In addition, signals of low intensity are observed between these two features. The spectrum is devoid of any hyperfine structure or half-field signal and does not show any appreciable temperature dependence. Analogous spectra have also been observed for other ferromagnetic chain copper complexes with oxalate[17] and *syn-anti* carboxylate bridges.[4] The frozen methanol solution spectrum of **3** at 100 K is typical of electronically isolated Cu^{II} species, thus suggesting that the chain structure is not retained in dilute methanol solution or that the magnetic exchange interaction does not appreciably affect the EPR spectrum.

The magnetic properties of the complexes **1**−**3** are given in Figure 2 in the form $\chi_M T$ versus T. The $\chi_M T$ products per metal atom at 290 K for complexes **1**−**3** are 4.41, 1.15, and 0.425 cm^3·mol^{-1}·K, respectively, which correspond well with those expected for isolated metal ions. For complexes **1** and **2**, $\chi_M T$ continuously decreases upon cooling and reaches values, at 4.2 K, of 1.225 and 0.056 cm^3·mol^{-1}·K, respectively, thus revealing the existence of an antiferromagnetic exchange interaction between metal ions through the carboxylate bridging group. The occurrence of susceptibility maximum around 5 and 25 K for **1** and **2**, respectively, is the signature of the antiferromagnetic interaction. The absence of a Curie-like tail at the lowest temperatures allows one to assume the absence of impurities in these products. For **3**, the $\chi_M T$ product steadily increases when the temperature decreases to a value of 0.63 cm^3·mol^{-1}·K at 2 K, thus suggesting a weak ferromagnetic interaction between the copper(II) ions. The experimental magnetization values as a function of the applied field at 5 K are higher than those predicted by the Brillouin function for $S = 1/2$, thus confirming the existence of weak ferromagnetic interaction between copper(II) ions.

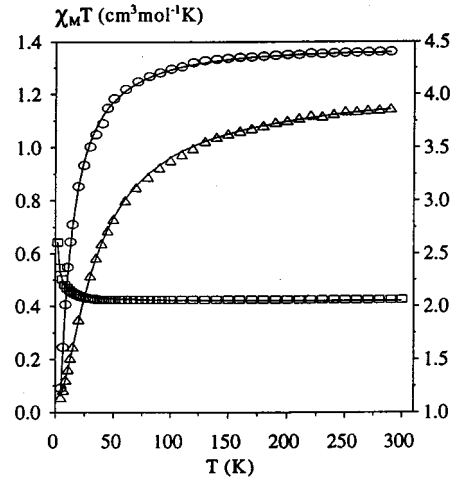

Figure 2. Magnetic plots ($\chi_M T$ vs T) of complexes: **1** (○) (right axis), **2** (△) (left axis) and **3** (□) (left axis)

We fitted the data of **1** using the analytical expression derived by Fisher for an infinite chain of classical spin scaled to $S = 5/2$;[18] for **2** we used the expression derived by Weng from calculations performed on ring systems of increasing lengths, where the nickel ion is assumed to be magnetically isotropic;[18] while the expression used to fit the magnetic data of **3** was that of Baker et al.,[18] which is based on the high-temperature Padé expansion technique.

Very good fits of the data of the complexes **1**−**3** to the corresponding theoretical equations can be obtained with $J = -0.91$ cm^{-1}, $g = 2.03$ (**1**); $J = -13.2$ cm^{-1}, $g = 2.24$ (**2**); $J = 0.40$ cm^{-1}, $g = 2.11$ (**3**).

The difference in the magnitude and sign of the magnetic exchange interactions found for **1**, **2**, and **3** can be satisfactorily explained in terms of the conformation of the bridge and the interaction between the d orbitals of the metal centre and the bridge. It is noteworthy that despite the larger separations found in complexes containing *anti-anti* bridges this configuration is more favourable for transmitting the interaction through the carboxylate bridge than the *syn-anti* one. The reason of these different magnetic behaviours lies in the fact that the contributions of the 2p oxygen orbitals belonging to the magnetic orbital centred on the metal ions are much more favourably oriented to give an effective overlap in the *anti-anti* than in the *syn-anti* configuration (see Scheme 1), thus leading to stronger magnetic exchange couplings.

In good accord with this, complexes **1** and **2** exhibit significant antiferromagnetic couplings with J values that are larger than those observed for singly bridged *syn-anti* car-

boxylate Mn^{II}[19] and alternating *syn-anti* and *anti-anti* carboxylate chain Mn^{II} and Ni^{II} complexes.[20] The *J* value for complex **1** is much smaller than that of complex **2**. Nevertheless, to deal with comparable values, the $n^2|J|$ relation (*n* is the number of unpaired electrons on each paramagnetic centre) should be taken into account. From the *J* values of **1** and **2** and the $n^2|J|$ relation we see that $|J_{Ni}|$ (13.2 cm^{-1}) >> 25/4 $|J_{Mn}|$ (5.7 cm^{-1}), thus illustrating the ability of Ni^{II} as compared to Mn^{II} to yield antiferromagnetic interactions, everything being equal. Similar *J* values have been reported for Mn^{II} (−1.1 cm^{-1}) and Ni^{II} (14 cm^{-1}) complexes with 2,2′-bipyrimidine,[21,22] a ligand that has been shown to transmit intermediate magnetic exchange couplings. Several reasons may contribute to the higher efficiency of the superexchange for the nickel(II) complex: (i) the larger spin delocalization on the bridge in the case of the Ni^{II}, since the energies of the $3d_{Ni}$ orbitals are lower and the M−O distances generally shorter than those of the Mn^{II}; (ii) small structural differences affecting either the carboxylate bridges or M^{II}−N,O bond lengths, and (iii) the possibility of more ferromagnetic contributions in the case of Mn^{II}.

In the case of **3**, the copper(II) ion exhibits a tetragonal elongated geometry, in which the unpaired electron is adequately described by a $d(x^2-y^2)$ orbital pointing toward the nitrogen and oxygen atoms of the basal equatorial plane, O(11)N(1)O(13)N(7). In light of the structural features of **3**, it is evident that these copper(II) orbitals are mismatched for interaction to take place between them through the carboxylate group, since the exchange pathway Cu−O−C−O−Cu involves an equatorial position on one copper [$d(x^2-y^2)$ direction] and an axial position on the other copper atom [$d(z^2)$ direction]. Departures from the idealized symmetry might allow some mixture with the $d(z^2)$ orbital, but in any case the overlap would be very weak. This would lead to a negligible antiferromagnetic contribution so that the ferromagnetic one becomes predominant. It should be noted that other carboxylate-bridged copper complexes having similar topology of the bridges also exhibit weak ferromagnetic interactions.[17]

Experimental Section

General: Elemental analyses were carried out with a Fisons-Carlo Erba analyzer, model EA 1108. − IR: Perkin−Elmer 983 G (KBr pellets). − Variable-temperature magnetic susceptibility data of **1** and **2** were collected on powdered samples of the compounds with the use of a pendulum-type magnetometer (MANICS DSM8) equipped with a helium continuous-flow cryostat working in the 300−4.2 K range and a Drusch EAF 164E electromagnet, whereas those of **3** (2−290 K) were obtained with a SQUID-based sample magnetometer using a Quantum Design Model MPMS instrument. Data were corrected for the diamagnetism of the ligands using Pascal′s constants. − EPR: Bruker ESP 300E (solid state: 300 and 100 K, methanol solution: 110 K).

Preparation of [M(HL)(hfac)] (1−3): These complexes were all prepared using the same method as described in detail for complex **1** as an example. This complex was prepared by refluxing 2-imidazolecarboxaldehyde (0.15 g, 1.56 mmol) and β-alanine (0.14 g, 1.56 mmol) for 1 h in 30 mL of an MeOH/H_2O mixture (4:1, v/v). To the cold, filtered yellow solution was added $Mn(hfac)_2$ (0.73 g, 1.56 mmol) in 30 mL of MeOH dropwise with stirring. The resulting yellow solution was kept at room temperature for 2 d and provided yellow prism-like crystals, which were filtered and air-dried. Yield: 0.60 g (90%). − $C_{12}H_9F_6MnN_3O_4$ (427.93): calcd. C 33.66, H 2.12, N 9.81; found C 33.49, H 1.96, N 10.15. − IR (KBr): $\tilde{\nu}$ = 3141 cm^{-1} (N_{im}−H), 1649, 1602 (C=O), 1257, 1217, 1144 (F−C).

2: Green powder. − Yield: 0.54 g (80%). − $C_{12}H_9F_6N_3NiO_4$ (431.71): calcd. C 33.41, H 2.10, N 9.75; found C 33.79, H 1.91, N 9.45. − IR (KBr): $\tilde{\nu}$ = 3137 cm^{-1} (N_{im}−H), 1649, 1600 (C=O), 1259, 1221, 1144 (F−C). − Powder X-ray diffraction:[23] monoclinic, *Pc*, *a* = 11.900(63), *b* = 8.462(24), *c* = 16.578(104) Å, β = 102.92(44)°.

3: Green plate-like crystals. − Yield: 0.44 g (65%). − $C_{12}H_9CuF_6N_3O_4$ (436.54): calcd. C 33.03, H 2.08, N 9.64; found C 32.98, H 2.09, N 9.53. − IR (KBr): $\tilde{\nu}$ = 3142 (N_{im}−H), 1664, 1625 (C=O), 1259, 1209, 1141 (F−C).

X-ray Crystallographic Study: Crystallographic data are listed in Table 2. The unit-cell parameters were determined and the data collected with a Rigaku AFC7S diffractometer at −80°C for complex **1** and with a Siemens P4 diffractometer at 20°C for **3**. The data were corrected for Lorentz polarisation effects and for dispersion, and an empirical absorption correction, using the programs TEXSAN[24a] and SHELXTL V5[24b] for **1** and **3**, respectively. The structures were solved by Direct methods using the SHELXS-86 program[24c] and refined (full-matrix least squares on F^2) by using the SHELX-97 and SHELXL-93 programs.[24d] For **1**, all non-hydrogen atoms were refined anisotropically, while for **3**, all non-hydrogen atoms were refined anisotropically except the F atoms, which were disordered and refined isotropically. In both cases, H atoms were included in calculated positions and treated as riding atoms using the SHELX-97 (for **1**) and SHELXL-93 (for **3**) default parameters.

Table 2. Crystal data and structure refinement for **1** and **3**

	Complex **1**	Complex **3**
Molecular formula	$C_{12}H_9N_3O_4F_6Mn$	$C_{12}H_9N_3O_4F_6Cu$
Mass	428.16	436.76
Unit-cell dimensions		
a [Å]	11.797(3)	11.290(5)
b [Å]	8.611(3)	8.685(5)
c [Å]	16.564(3)	16.799(5)
β [°]	104.49(3)	105.598(5)
Z	4	4
$d_{calcd.}$ [g cm^{-3}]	1.746	1.829
Crystal system	monoclinic	monoclinic
Space group	*P*2(1)/*c* (no. 14)	*P*2(1)/*c* (no. 14)
Crystal size [mm]	0.15 × 0.12 × 0.06	0.40 × 0.30 × 0.06
Absorption coeff. [mm^{-1}]	0.899	1.468
θ range data collection [°]	2.54−25.00	1.87−30.00
Reflections collected	3016	5663
Independent reflections	2868	4440
Data/restraints/parameters	2868/6/235	4419/0/295
*R*1 [*I* > 2 (*I*)]	0.0714	0.0442
w*R*2 [*I* > 2 (*I*)]	0.1433	0.1203
Goodness-of-fit on F^2	1.033	0.731

Acknowledgments

Financial support from the Dirección General de Investigación Científica y Técnica (DGICYT) through project PB94−0764 is

acknowledged. We thank Dr. A. Mari from the Laboratoire de Chimie de Coordination (C.N.R.S.), Toulouse, France, for his contribution to the magnetic measurements. Academy of Finland is acknowledged by R. K.; M. G. thanks the Ministère de L′Education Nationale Marocaine − Enseignement Superieur for a grant.

[1] *Manganese Redox Enzymes* (Ed.: V. L. Pecoraro), VCH, New York, **1992**, p. 1−28.
[2] K. Wieghardt, *Angew. Chem.* **1989**, *101*, 1179−1198; *Angew. Chem. Int. Ed. Engl.* **1989**, *28*, 1153−1172.
[3] E. Coronado in *Magnetic Molecular Materials* (Eds.: D. Gatteschi, O. Khan, J. E. Miller, F. Palacio), Nato ASI Series, E198, Kluwer Academic Publisher, Dordrecht, **1991**, p. 267−279.
[4] E. Colacio, J. M. Dominguez-Vera, J. P. Costes, R. Kivekäs, J. P. Laurent, J. Ruiz, M. Sundberg, *Inorg. Chem.* **1992**, *31,* 774−778 and references therein.
[5] E. Colacio, J. M. Dominguez-Vera, R. Kivekäs, J. M. Moreno, A. Romerosa, J. Ruiz, *Inorg. Chim. Acta* **1993**, *212*, 115−121 and references therein.
[6] Z. N. Chen, S. X. Liu, J. Qiu, Z. M. Wang, J. L. Huang, W. X. Tang, *J. Chem. Soc., Dalton Trans.* **1994**, 2989−2993.
[7] J. P. Costes, F. Dahan, J. P. Laurent, *Inorg. Chem.* **1985**, *24,* 1018−1022.
[8] M. Kato, Y. Muto, *Coord. Chem. Rev.* **1988**, *92*, 45.
[9] M. Inoue, M. Kubo, *Inorg. Chem.* **1970**, *9*, 2310−2314.
[10] D. K. Towle, S. K. Hoffmann, W. E. Hatfield, P. Singh, P. Chaudhuri, *Inorg. Chem.* **1988**, *27*, 394−399.
[11] J. E. Davies, B. M. Gatehouse, K. S. Murray, *J. Chem. Soc., Dalton Trans.* **1973**, 2523−2527.
[12] K. K. Nanda, A. W. Addison, E. Sinn, L. K. Thompson, *Inorg. Chem.* **1996**, *35*, 5966−5967.
[13] J. A. Bonadies, M. L. Kirk, M. S. Lah, D. P. Kessissoglou, W. E. Hatfield, V. L. Pecoraro, *Inorg. Chem.* **1989**, *28*, 2037−2044.
[14] N. Aurangzeb, C. E. Hulme, C. A. McAuliffe, R. G. Pritchard, M. Watkinson, A. García-Deibe, M. R. Bermejo, A. Sousa, *J. Chem. Soc., Chem. Commun.* **1992**, 1524−1526.
[15] M. A. Martínez-Lorente, J. P. Tuchagues, V. Pétrouléas, J. M. Savariault, R. Poinsot, M. Drillon, *Inorg. Chem.* **1991**, *30*, 3587−3589.
[16] C. J. O′Connor, D. P. Freyberg, E. Sinn, *Inorg. Chem.* **1979**, *18*, 1077−1088.
[17] J. Suárez-Varela, J. M. Dominguez-Vera, E. Colacio, J. C. Avila-Rosón, M. A. Hidalgo, D. Martín-Ramos, *J. Chem. Soc., Dalton. Trans.* **1995**, 2143−2146 and references therein.
[18] O. Kahn, *Molecular Magnetism*, VCH, New York, **1993**.
[19] V. Tangoulis, G. Psomas, C. Dendrinou-Samara, C. P. Raptopoulou, A. Terzis, D. P. Kessissoglou, *Inorg. Chem.* **1996**, *35*, 7655−7660.
[20] J. J. Borrás-Almenar, E. Coronado, C. J. Gómez-García, L. Ouahab, *Angew. Chem.* **1993**, *105*, 637−639; *Angew. Chem. Int. Ed. Engl.* **1993**, *32,* 561−563.
[21] G. De Munno, M. Julve, F. Lloret, A. Derory, *J. Chem. Soc., Dalton Trans.* **1993**, 1179−1184.
[22] G. De Munno, R. Ruiz, F. Lloret, J. Faus, R. Sessoli, M. Julve, *Inorg. Chem.* **1995**, *34*, 408−411.
[23] D. Martín-Ramos, *PLV, A program for PXRD evaluation*, Departamento de Mineralogia y Petrologia, Universidad de Granada, E-18071 Granada, Spain, **1995**; available from the author.
[24] [24a] *TEXSAN: Single Crystal Structure Analysis Software*, Molecular Structure Corp., The Woodlands, TX, USA, **1993**. − [24b] *SHELXTL PC, version 5.0*, Siemens Analytical X-ray Instruments, Madison, WI, **1995**. − [24c] *SHELXS-86:* G. M. Sheldrick, *Acta Crystallogr.* **1990**, *A46,* 467−473. − [24d] G. M. Sheldrick, *SHELXL-93* and *SHELX-97*, Universität Göttingen, **1993** and **1997**.

Received July 9, 1998
[I98223]